

Excitation of longitudinal and Lamb waves in plates by edge-mounted transducers

D.W. Greve

Department of Electrical and Computer Engineering
Carnegie Mellon University
Pittsburgh, PA 15213
dg07@andrew.cmu.edu

Peng Zheng

Department of Physics
Carnegie Mellon University
Pittsburgh, PA 15213

I.J. Oppenheim

Department of Civil and Environmental Engineering
Carnegie Mellon University
Pittsburgh, PA 15213

Abstract—Lamb waves have been extensively studied for the detection of flaws in plate-like structures. However operation at low fd products is usually recommended in order to eliminate the complications of multiple Lamb modes, and low fd products lead to reduced scattering from small defects. Here we explore the generation of waves at higher fd products. We explore the transition between the generation of multiple Lamb modes and the generation of a train of nearly longitudinal pulses. We also investigate the transfer of energy from the leading to trailing pulses along with the scattering of the pulse train by simulated defects.

Keywords- Lamb waves, longitudinal waves, flaws

I. INTRODUCTION

Considerable research has been directed at the detection of defects in plate-like structures using Lamb waves. This application has been motivated by the fact that pulses formed from Lamb waves propagate with low attenuation for large distances in plates. However, the existence of multiple Lamb wave modes presents a significant complication. Lamb waves are typically excited by transducers mounted on the surface of the plate; and numerous modes are generated when the frequency-thickness product fd exceeds, say, 3 MHz·mm (in metals such as steel or aluminum). As a result, many researchers have recommended working at low fd products so that only a small number of modes are excited [1-3] and other work has concerned the development of transducers that selectively emit particular modes [4-6]. However, limiting operation to low frequencies is not a completely satisfactory solution because scattering becomes weaker and the resolution is degraded when the defect is small compared to the wavelength [7].

In this paper we consider the creation of waves in plates by edge excitation at fd products that correspond to multiple Lamb wave modes. For relatively low values of fd it is clear that Lamb wave modes will be generated while at large fd we will encounter longitudinal waves. We consider here intermediate fd where a pulse train of nearly longitudinal

waves is generated. These “trailing pulses” are well known and have been explained in the literature. We will examine the transition from Lamb wave generation to the formation of nearly longitudinal waves and trailing pulses. In addition we will examine the transport of energy from leading to trailing pulses and the interaction of these trailing pulses with cracks. The results suggest that these nearly longitudinal waves may be an attractive option for flaw detection.

II. TRANSITION FROM LAMB TO LONGITUDINAL WAVES

In this section, we use finite element simulation to examine the transition from Lamb wave to longitudinal wave generation. Figure 1 shows the geometry under consideration. A plate of thickness d is excited by a force normal to the edge. A good approximation to this situation results when a plate is excited by a conventional piezoelectric transducer using grease coupling.



Figure 1. Plate of thickness d excited by a time-dependent force $F_x(t)$ normal to the edge.

Simulations were performed in the plane-strain structural mechanics mode of COMSOL 3.2 for a plate 2 cm thick and 35 cm long. A force in the x direction with the time dependence $F(t) = F_0 \sin(2\pi ft) \sin(2\pi ft / 10)$ for five periods ($t < 5/f$) was applied to the left edge of the model. Material parameters (Young's modulus $E = 2 \times 10^{11}$ N/m², Poisson ratio 0.33, density 7850 kg/m³, mass damping parameter 0.001 and stiffness damping parameter 10^{-9}) were chosen appropriate for steel. A transient (time dependent) analysis was performed using a step size of $1/10f$. The mesh parameters for simulations at $f > 600$ kHz were chosen to give a maximum element size of 0.2 cm, resulting in approximately 13200 elements, whereas

slightly larger element sizes (0.25 cm) were used at lower frequencies. One simulation at 1 MHz was repeated using a smaller element size of 0.12 cm in order to verify that the mesh size for other simulations was sufficiently small.

We first consider the effect of pulse center frequency on wave generation. Figure 2 shows the effect of launching a wave with edge excitation at various frequencies by plotting the particle displacement (in the x direction) in the plate at $t = 50 \mu\text{s}$. At low frequencies (up to about 450 kHz) the wavefront velocity is significantly slower than the bulk wave longitudinal velocity ($c_l = 5.9 \times 10^5 \text{ cm/sec}$), and particle displacements are similar to those for low-order symmetric Lamb modes. Simulations have also been performed for longer propagation times, up to $t = 175 \mu\text{s}$ in a plate 85 cm long (not shown). In these simulations separation into multiple Lamb modes with different propagation velocity can be clearly observed. For example, at 200 kHz at least two distinct Lamb modes are observed, a faster mode with group velocity of about $4.6 \times 10^5 \text{ cm/sec}$, and a slower mode with group velocity about $3.4 \times 10^5 \text{ cm/sec}$. These particular modes can be identified as S1 and S2 modes, respectively, and both of these Lamb wave modes are predicted to be present at $fd = 4 \text{ MHz}\cdot\text{mm}$.

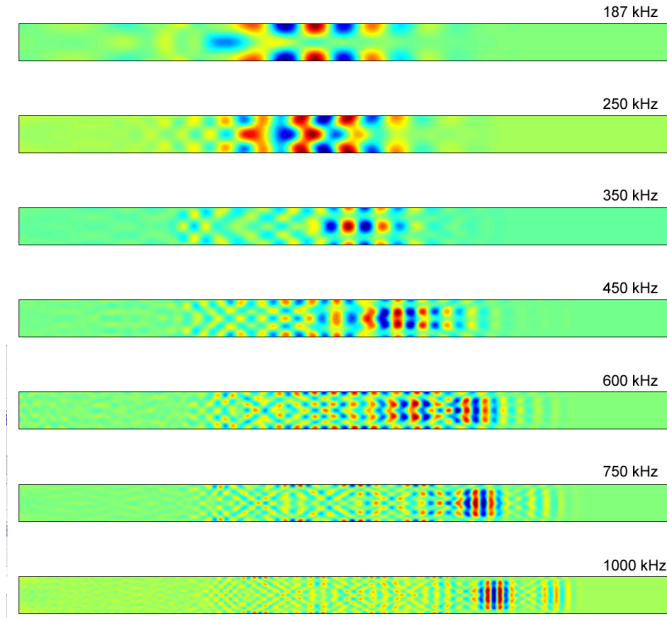


Figure 2. Simulated x displacement at $t = 50 \mu\text{s}$ after launching a wave with various center frequencies.

At higher fd products, theory predicts that a greater number of Lamb wave modes will be present with a considerable range of group velocities, and as a result one might expect a long pulse train with complex character. However, the simulation results in Figure 2 for higher frequency excitations show particle velocities that are nearly uniform across the thickness of the plate, traveling with a group velocity essentially equal to the bulk wave longitudinal velocity. This behavior is fully established at 750 kHz and above ($fd = 15 \text{ MHz}\cdot\text{mm}$).

At these higher frequencies a leading pulse travels at the longitudinal velocity but that leading pulse decays in amplitude

and a trailing pulse forms behind it. Figure 3 shows the evolution of the pulse train at 1000 kHz. The decay of the leading pulse and growth of a trailing pulse is clearly visible. The formation of a third trailing pulse is also visible in this figure.



Figure 3. Simulations showing evolution of a pulse train excited with a center frequency of 1000 kHz. The leading nearly-longitudinal pulse decays in amplitude while trailing pulses gain in amplitude. The color indicates the x displacement.

The formation of trailing pulses is well known; these have been referred to as “secondary echoes produced by split-off transverse waves [8]”. The trailing pulses appear because glancing incidence of a longitudinal wave on a surface results in reflection of a transverse wave with lower propagation velocity. That transverse wave then reflects from the opposite surface and is converted back into a delayed longitudinal wave. The angle at which the transverse wave is reflected is determined by the longitudinal and transverse velocities; this leads to an expression for the time delay between pulses [8]

$$\Delta t = \frac{d}{c_t \cos \theta} - \frac{d \tan \theta}{c_l} \quad (1)$$

where d is the thickness of the plate. The predicted delay is $4.9 \mu\text{s}$ for a plate 2 cm in thickness, in good agreement with the simulations.

Wave propagation theory accurately predicts the delay between trailing pulses, but does not predict the transition from Lamb waves generation to trailing pulses. Our simulations show that this transition occurs at relatively small values of $fd = 15 \text{ MHz}\cdot\text{mm}$. In the following we report additional results from the simulations concerning the transfer of energy from the leading to trailing pulses and scattering from cracks.

III. PROPAGATION OF TRAILING PULSES

We first consider the transfer of energy from leading to trailing pulses. Figure 4 shows the x displacement averaged

across the plate thickness for several locations. The average x displacement is roughly proportional to the voltage measured by a transducer at each location. We see that the leading pulse decays with distance and that the following pulses gain in amplitude.

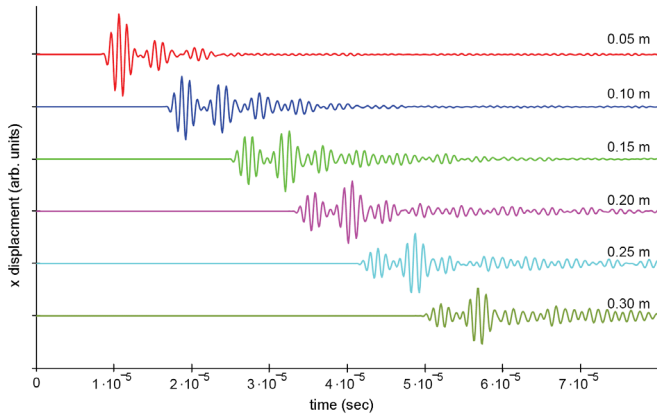


Figure 4. Plot of the simulated average x displacement through the thickness of the plate at various distances from the excited edge (center frequency = 1000 kHz).

Additional simulations at different frequencies have been performed, and Table I shows the propagation distance at which the leading and second pulses become equal in amplitude. This distance increases with the fd product. At lower center frequencies the pulses are wider and begin to overlap, while at higher frequencies at least five distinct trailing pulses can be seen after a propagation distance of 0.30 m. Energy is transferred from leading to trailing pulses but the individual pulses retain their shape without significant broadening.

TABLE I. PROPAGATION DISTANCE AT WHICH LEADING AND FIRST TRAILING PULSES ARE EQUAL IN AMPLITUDE.

frequency [MHz]	fd [mm·MHz]	distance [m]
0.75	15	< 0.1
1.00	20	< 0.15
1.25	25	0.2
1.5	30	0.3

Finally we consider scattering of nearly-longitudinal waves from a crack. It is possible that scattering from a crack would result in mode conversion to Lamb wave modes, which would make detection of cracks substantially more difficult. In order to observe such mode conversion, were it to occur, simulations were performed to include the effect of scattering from a part-thickness slot 1 mm wide and with varying depth. The simulations were performed with a center frequency of 1 MHz for a plate 0.4 m long with a crack located 0.2 m from the left edge at which the excitation was applied. Figure 5 shows a nearly-longitudinal wave approaching the crack (top, $t = 30 \mu\text{s}$) and the transmitted and reflected waves (bottom, $t = 50 \mu\text{s}$).

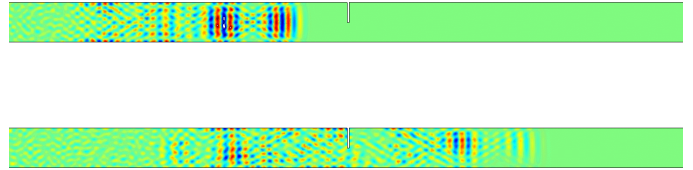


Figure 5. A pulse train approaching a half-thickness slot (top, $t = 30 \mu\text{s}$) and after reflection from the slot (bottom, $t = 50 \mu\text{s}$). The center frequency was 1000 kHz.

Figure 6 shows the average x displacement as a function of time at two locations, $x = 0.10 \text{ m}$ and $x = 0.30 \text{ m}$, respectively, symmetrically positioned with respect to the crack. Figure 6 (top) shows the incident wave approaching the first location ($x = 0.10 \text{ m}$) at $t \sim 20 \mu\text{s}$, and a wave reflected from the crack approaching that same location on its return path at $t \sim 50 \mu\text{s}$. Figure 11 (bottom) shows the transmitted wave, after having passed the scatterer, reaching the second location ($x = 0.30 \text{ m}$) at $t \sim 50 \mu\text{s}$ with nearly the same amplitude and shape as the reflected wave returning to the first location. In both reflected and transmitted waves, the second pulse is larger than the leading pulse, consistent with the simulations for a total travel distance of 0.30 m without a crack as shown in Fig. 4. The expected trend with crack depth is observed, with the ratio of reflected wave amplitude increasing monotonically with increasing crack depth (not shown).

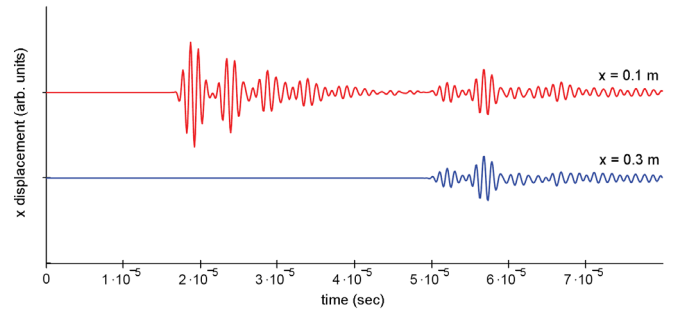


Figure 6. Simulation of the average x displacement as a function of time at two locations (center frequency 1000 kHz).

IV. EXPERIMENTAL VERIFICATION

In this section we report experiments verifying the simulation results presented above. Experiments were performed using a steel plate 19 mm thick and 30.5 cm long. Piezoelectric transducers consisting of 5A4E PZT (Piezo Systems, Cambridge, MA), $15 \times 15 \times 1 \text{ mm}$ with a lead backing 3 mm thick, were attached at opposite edges. One transducer was driven with a voltage waveform with the same functional form used in the simulations reported above. The transducer was excited and the received waveforms at both transducers were recorded using a National Instruments PXI-6115 DAQ board. The center frequency for the pulse excitation was 2.2 MHz, corresponding to $fd = 42 \text{ MHz}\cdot\text{mm}$.

Figure 7a shows the waveform received at the opposite side from the transmitting transducer. The trailing pulses are clearly visible and at least five can be distinguished. Figure 7b shows

the waveform returned to the transmitting transducer after cutting a slot 3 mm wide and 5.7 mm in depth midway along the propagation path. A pulse train reflected from the slot is

observed beginning at $t = 50 \mu\text{s}$ and a larger amplitude pulse train reflected from the opposite wall appears at $t = 105 \mu\text{s}$.

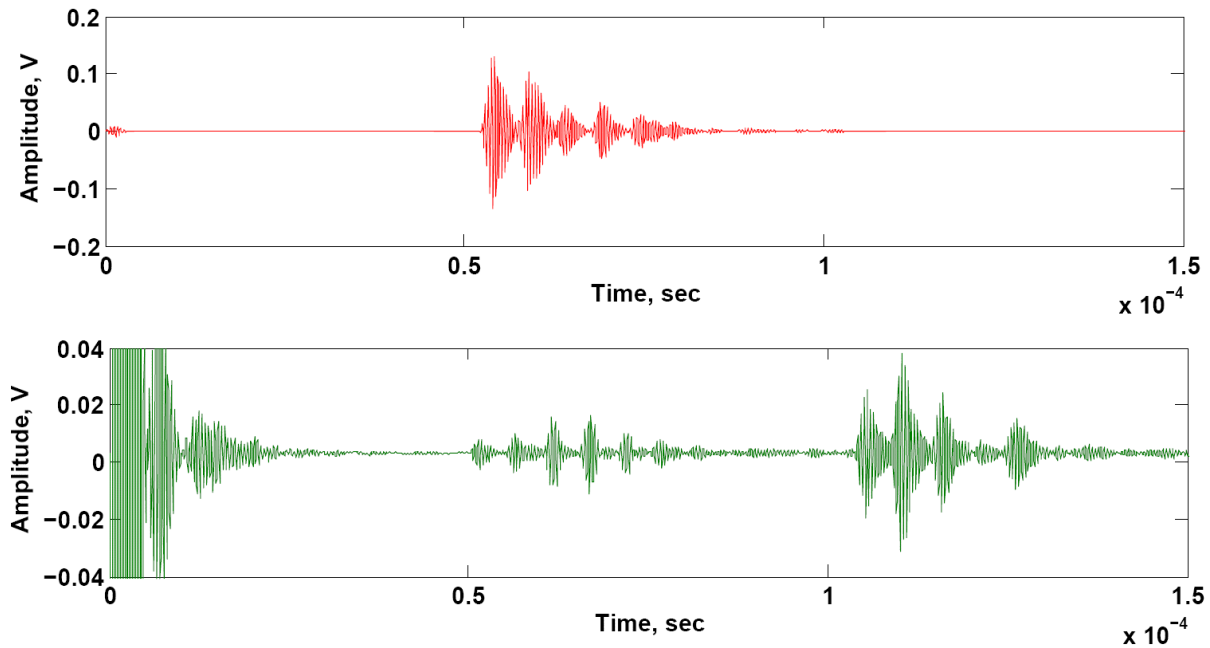


Figure 7. Experimental observations of trailing pulses: (top) received signal after a propagation path length of 0.3 m; and (bottom) reflected signal from a part-thickness slot (center frequency 2.2 MHz).

V. CONCLUSIONS

We have examined the generation of waves in plates by force excitation normal to the edge as a function of pulse center frequency. Both simulations and experiment show that multiple Lamb modes are created at low fd products, while for $fd > 15$ mm·MHz a nearly longitudinal pulse is generated which is followed by several trailing pulses. During propagation energy is transferred from the leading pulse to trailing pulses. Our simulations show that the rate of transfer of energy from leading to trailing pulses decreases with increasing center frequency. Both experimental results and simulations show that the pulse train retains its integrity over distances of at least one meter. We have also studied the interaction of a pulse train with a slot, simulating scattering from a partial-thickness crack. Both transmitted and reflected pulse trains are observed and there is no sign of mode conversion to Lamb waves. These nearly-longitudinal waves are attractive as an alternative to Lamb waves for the detection of defects in plate-like structures. An important advantage of the nearly-longitudinal modes is the shorter wavelength which will result in enhanced scattering from small defects. Reflection of a pulse train rather than a single pulse will complicate the interpretation of data. This complication may be acceptable in order to take advantage of higher scattering amplitude.

VI. ACKNOWLEDGEMENTS

The authors gratefully acknowledge support from Bombardier Total Transit Systems and the Pennsylvania

Infrastructure Technology Alliance and from the National Science Foundation under grant CMS-0329880. Any opinions, findings, and conclusions or recommendations expressed in this material are those of the authors and do not necessarily reflect the views of the National Science Foundation.

VII. REFERENCES

- [1] D. N. Alleyne, and P. Cawley, "Optimization of Lamb wave inspection techniques", *NDT & E Int.* vol. 25, pp. 11-22, 1992.
- [2] J.-B. Ihn and F.-K. Chang, "Detection and monitoring of hidden fatigue crack growth using a built-in piezoelectric sensor/actuator network: I. Diagnostics," *Smart Mater. Struct.* vol. 13, pp. 609-620, 2004.
- [3] S.G. Pierce, B. Culshaw, G. Manson, K. Worden, W.J. Staszewski, "Application of ultrasonic Lamb wave techniques to the evaluation of advanced composite structures," *Proceedings of the SPIE*, vol. 3986, pp. 93-103, 2000.
- [4] J.L. Rose, S. Pelts, and M. Quarry, "A comb transducer model for guided wave NDE," *Ultrasonics* vol. 36, pp. 163-168, 1998.
- [5] W. Zhu and R.L. Rose, "Lamb wave generation and reception with time-delay periodic linear arrays: A BEM simulation and experimental study," *IEEE Trans. Ultrasonics, Ferroelectrics, and Frequency Control* vol. 46, pp. 654-664, 1999.
- [6] V. Giurgiutiu, "Lamb Wave Generation with Piezoelectric Wafer Active Sensors for Structural Health Monitoring," *Proceedings of the SPIE-Smart Structures and Materials 2003: Smart Structures and Integrated Systems* vol. 5056, pp. 111-122, 2003.
- [7] P. Fromme, B. Masserey, and M. B. Sayir, "On the Detectability of Fatigue Crack Growth at Fastener Holes Using Guided Waves," *Review of Progress in Quantitative Nondestructive Evaluation* vol 22, pp. 189-196, 2003.
- [8] J. Krautkramer and H. Krautkramer, *Ultrasonic Testing of Materials*, 4th fully revised ed., Springer-Verlag, 1990, pp. 283-286.